

Polarization rotation effects in atomic sodium vapor

P. F. Liao and G. C. Bjorklund

Bell Telephone Laboratories, Holmdel, New Jersey 07733

(Received 8 December 1977)

Polarization rotation effects in atomic sodium vapor are studied both experimentally and theoretically. Two pulsed dye laser beams propagate collinearly through a cell containing sodium vapor. The direction of polarization of a linearly polarized dye laser beam of frequency ω_1 is found to be rotated by a circularly polarized beam of frequency ω_2 . This rotation is due to the difference in refractive index at ω_1 for right and left circularly polarized light which is produced by the circularly polarized beam. When $\omega_1 + \omega_2$ is tuned near the 3S-5S two-photon transition of atomic sodium, this difference is primarily due to the dispersion associated with the two-photon transition. Other sources of polarization rotation which were identified include (i) real transfers of population to excited atomic levels due to collisionally induced transitions and (ii) optically induced atomic energy-level shifts. The theory includes both the effects of two-photon dispersion and optically induced energy shifts. The application of the two-photon polarization rotation effect as a fast, optically controlled shutter or modulator and as a sensitive detection technique for two-photon spectroscopy are briefly discussed.

I. INTRODUCTION

We have recently described some preliminary measurements¹ of a polarization rotation effect which is produced by the dispersion associated with a nearly resonant two-photon transition in an atomic vapor. The polarization of a linearly polarized dye laser beam of frequency ω_1 was found to be rotated by a circularly polarized laser beam of frequency ω_2 when $\omega_1 + \omega_2$ was tuned near the 3S - 5S two-photon transition frequency of atomic sodium. The observation of this effect in potassium vapor has also been reported by V. M. Arutyunyan *et al.*² and its application for purposes of Raman spectroscopy has been discussed by D. Heiman *et al.*³ A similar polarization rotation effect which is useful for saturation spectroscopy has recently been reported by Wieman and Hänsch.⁴

In this paper we report the results of more detailed experiments on this rotation effect in atomic sodium vapor. In addition to two-photon dispersion, we have been able to identify two other sources of polarization rotation. These are (1) real transfers of population to excited atomic levels due to collisionally induced transitions and (2) optically induced atomic energy-level shifts. We also give a detailed theoretical derivation of the effect which neglects the effects of collisions and spontaneous emission but includes both the energy shifts and two-photon dispersion.

The two-photon polarization rotation effect is potentially useful in two respects. First, when combined with a polarizer, a fast, optically controlled shutter or modulator is obtained.⁵ Because of the great transparency of atomic vapors, such a shutter can be used over a wide range of the electromagnetic spectrum from the far-in-

frared to the vacuum ultraviolet. Second, the rotation effect can be used as a sensitive detection technique for high-resolution two-photon spectroscopy. This technique may prove particularly useful in those systems for which two-photon transitions are not easily monitored by means of fluorescence.

The two-photon polarization rotation effect is a result of the selection rules for two-photon absorption. A particularly simple case is an S-to-S transition of an atomic alkali vapor. The selection rules⁶ for this type of two-photon transition are such that the absorption of circularly polarized photons requires that the two photons must have opposite senses of circular polarization. Hence, while a right circularly polarized control laser beam at frequency ω_2 will induce the alkali atom to exhibit an absorption resonance at $\Omega - \omega_2$ for left circularly polarized light, where Ω is the two-photon transition frequency, no such absorption resonance will be present for right circularly polarized radiation. The S-to-S transition will affect only one of the two circularly polarized components of a linearly polarized signal beam at ω_1 . Associated with the two-photon absorption resonance is a dispersion susceptibility which is directly related to the absorption through the Kramers-Kronig relationships. By correctly adjusting ω_2 such that $\Omega - \omega_2$ is nearly equal to ω_1 , this two-photon dispersion can produce considerable phase shift for the left circularly polarized component of ω_1 while avoiding significant absorption of either beam. The right circularly polarized component propagates unaffected. The result is a simple rotation of the direction of polarization of the beam at ω_1 . In general, the combined effects of the absorptive and dispersive parts of the two-photon susceptibility will cause

the signal beam to become elliptically polarized. Note that the induced resonance occurs at $\Omega - \omega_2$, and therefore this resonance frequency can be simply adjusted with the control-laser frequency, ω_2 . This ability to tune the resonance frequency is important since it can considerably relax the requirement of a chance coincidence with a resonant atomic transition that has restricted the usefulness of many phenomena associated with single-photon transitions.⁷

Single-photon transitions are also a source of polarization rotation. The dispersion associated with these transitions is modified by the control laser beam. The modification occurs because the control beam produces optical Stark shifts of the atomic levels. Bonch-Bruevich *et al.*⁸ have reported the observation of optical birefringence due to optically induced level shifts produced by linearly polarized light. Circular polarization of the control beam light produces changes in the single-photon susceptibility which results in optical activity and circular dichroism. In the following section we present a theory which treats both two-photon dispersion and the level shifts in a unified manner to obtain explicit expressions for the rotation effect for *S*-to-*S* two-photon transitions. Section III describes the experimental apparatus and the experimental results are given in Section IV.

II. THEORY

The theory of coupled three-level systems has been extensively discussed in the literature.⁹ We shall extend this theory to the four level system shown in Fig. 1, in order that we may correctly

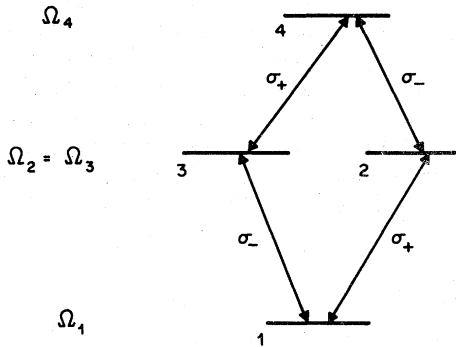


FIG. 1. Energy-level diagram: The four Zeeman sublevels have the energies indicated and are connected by matrix elements for circularly polarized light as shown.

account for the possibility of coupling the atomic system to radiation containing both right- and left-handed circularly polarized components, and to include simultaneously the effects of both single-photon and two-photon dispersion. The levels 1-4 are the appropriate Zeeman sublevels of the atomic system such that levels 1 and 3 are connected to levels 2 and 4 by right circularly polarized transitions and levels 1 and 2 are connected to levels 3 and 4 by left circularly polarized transitions. In the absence of external fields the levels 2 and 3 are degenerate in energy.

We assume the atom is irradiated by a strong circularly polarized control laser beam whose electric field is

$$\vec{E}_2 = \mathcal{E}_2(\hat{x} \cos \omega_2 t + \hat{y} \sin \omega_2 t) \quad (1)$$

and a weak, linearly polarized signal beam

$$\begin{aligned} \vec{E}_1 &= \mathcal{E}_1 \hat{x} \cos \omega_1 t \\ &= \mathcal{E}_{1R}(\hat{x} \cos \omega_1 t + \hat{y} \sin \omega_1 t) \\ &\quad + \mathcal{E}_{1L}(\hat{x} \cos \omega_1 t - \hat{y} \sin \omega_1 t). \end{aligned} \quad (2)$$

The assumption of a weak signal-probe laser beam has been made to simplify the theory. The interaction of the control beam with the atomic system will be treated exactly and the weak signal beam will be treated as a perturbation.

In Ref. 10, a derivation of the two-photon susceptibility is given in which the signal and control beams may have comparable intensities. That derivation was concerned with the region in the immediate vicinity of the two-photon resonance, and hence the effects of optically induced level shifts on single-photon transitions were not included. Polarization rotation effects, however, are due to the dispersive part of the two-photon susceptibility and this dispersion extends to regions which are significantly detuned from the two-photon resonance. In these regions the effects of the optically shifted single-photon resonances can be comparable to the effects of the two-photon resonance. Therefore, we have extended the derivation of Ref. 10 to include the optically induced shifts of single-photon resonances.

The interaction of the strong control laser beam causes the initial unperturbed atomic states to change into new "adiabatic states"¹¹ or "dressed-atom states"¹² which consists of linear superpositions of the original unperturbed states. The new "adiabatic states" are obtained as follows. The Hamiltonian \mathcal{H} which describes the atom and the

interaction between the atom and the applied light is assumed to be of the form

$$\begin{aligned} \mathcal{H} &= \mathcal{H}_0 - \vec{P} \cdot \vec{E}_2 - \vec{P} \cdot \vec{E}_1 \\ &= \mathcal{H}_1 - \vec{P} \cdot \vec{E}_1 \end{aligned} \quad (3)$$

where \mathcal{H}_0 is the unperturbed atomic Hamiltonian, and \vec{P} is the electric-dipole-moment operator. The matrix elements of \vec{P} are

$$\mathcal{H}_1 = \begin{pmatrix} \hbar\Omega_1 & \mathcal{E}_2 P_{12} e^{-i\omega_2 t} & 0 & 0 \\ \mathcal{E}_2 P_{12} e^{+i\omega_2 t} & \hbar\Omega_2 & 0 & 0 \\ 0 & 0 & \hbar\Omega_3 & \mathcal{E}_2 P_{34} e^{-i\omega_2 t} \\ 0 & 0 & \mathcal{E}_2 P_{34} e^{+i\omega_2 t} & \hbar\Omega_4 \end{pmatrix}. \quad (5)$$

We now define the unitary operator

$$T = U e^{-i\Lambda t}, \quad (6)$$

where

$$\Lambda = \begin{pmatrix} 0 & 0 & 0 & 0 \\ 0 & \omega_2 & 0 & 0 \\ 0 & 0 & \omega_2 & 0 \\ 0 & 0 & 0 & 2\omega_2 \end{pmatrix}, \quad (7)$$

$$U = \begin{pmatrix} N_a & \alpha_a N_a & 0 & 0 \\ -\alpha_a N_a & N_a & 0 & 0 \\ 0 & 0 & N_b & \alpha_b N_b \\ 0 & 0 & -\alpha_b N_b & N_b \end{pmatrix}, \quad (8)$$

with

$$N_a = \frac{\eta_a}{[(P_{12} \mathcal{E}_2)^2 + \eta_a^2]^{1/2}}, \quad N_b = \frac{\eta_b}{[(P_{34} \mathcal{E}_2)^2 + \eta_b^2]^{1/2}}$$

$$\alpha_a = P_{12} \mathcal{E}_2 / \eta_a, \quad \alpha_b = P_{34} \mathcal{E}_2 / \eta_b$$

and

$$\begin{aligned} \eta_a &= \frac{1}{2} [(\Omega_{21} - \omega_2) + [(\Omega_{21} - \omega_2)^2 + 4(P_{12} \mathcal{E}_2)^2]^{1/2}], \\ \eta_b &= \frac{1}{2} [(\Omega_{43} - \omega_2) + [(\Omega_{43} - \omega_2)^2 + 4(P_{34} \mathcal{E}_2)^2]^{1/2}], \\ \Omega_{21} &= \Omega_2 - \Omega_1, \quad \Omega_{43} = \Omega_4 - \Omega_3. \end{aligned}$$

The equation of motion of the density matrix, ρ ,

$$\frac{\partial \rho}{\partial t} = \frac{i}{\hbar} [\rho, \mathcal{H}] \quad (9)$$

may be transformed to

$$\frac{\partial \rho'}{\partial t} = \frac{i}{\hbar} [\rho', \mathcal{H}'], \quad (10)$$

$$\vec{P}_{14} = \vec{P}_{41} = \vec{P}_{23} = \vec{P}_{32} = 0,$$

$$\vec{P}_{12} = \vec{P}_{21}^* = P_{12}(\hat{x} - i\hat{y}),$$

$$\vec{P}_{13} = \vec{P}_{31}^* = P_{13}(\hat{x} + i\hat{y}), \quad (4)$$

$$\vec{P}_{24} = \vec{P}_{42}^* = P_{24}(\hat{x} + i\hat{y}),$$

$$\vec{P}_{34} = \vec{P}_{43}^* = P_{34}(\hat{x} - i\hat{y}).$$

Using the rotating-wave approximation we obtain

where

$$\rho' = T \rho T^{-1} \quad (11)$$

and the effective Hamiltonian, \mathcal{H}' is given by

$$\begin{aligned} \mathcal{H}' &= T \mathcal{H} T^{-1} + \hbar \Lambda \\ &= T \mathcal{H}_1 T^{-1} + \hbar \Lambda - V, \end{aligned} \quad (12)$$

where

$$V = T(\vec{P} \cdot \vec{E}_1) T^{-1} \quad (13)$$

and $T \mathcal{H}_1 T^{-1} + \hbar \Lambda$ is diagonal with eigenvalues,

$$\begin{aligned} \lambda_1 &= \Omega_2 + \Omega_1 - \omega_2 - \lambda_2, \quad \lambda_2 = \eta_a + \Omega_1, \\ \lambda_3 &= \Omega_4 + \Omega_3 - 3\omega_2 - \lambda_4, \quad \lambda_4 = \eta_b + \Omega_3 - \omega_2. \end{aligned} \quad (14)$$

The states which are obtained with the transformation, T , are clearly the eigenstates of the Hamiltonian, \mathcal{H}' , which includes the unperturbed atomic Hamiltonian and the interaction with field \mathcal{E}_2 only. These eigenvalues are accurate provided that the rotating-wave approximation, which assumes $|\Omega_{21} - \omega_2| \ll \Omega_{21}$, is satisfied. Because of the adiabatic theorem of quantum mechanics,¹³ an atom which is initially in its ground state will remain in the ground adiabatic state if the field \mathcal{E}_2 is applied adiabatically and $\mathcal{E}_1 = 0$ (in the absence of relaxation processes). This adiabatic condition is given as

$$\left| \frac{\partial \mathcal{E}_2}{\partial t} \right| \ll |\Delta \omega \mathcal{E}_2| \quad (15)$$

when $\Delta \omega$ is the mistuning, $\Omega_2 - \Omega_1 - \omega_1$. Hence the terminology "adiabatic states" is particularly appropriate.

By treating the interaction term $-\vec{P} \cdot \vec{E}_1$ with first order perturbation theory we can solve Eq. (10) and obtain

$$\begin{aligned}
\rho'_{11} &\approx 1, \\
\rho'_{12} = \rho'_{21} &\approx N_a^2 \frac{P_{12} \mathcal{E}_{1R} e^{-i(\omega_{12})t}}{\lambda_{21} - \hbar \omega_{12}}, \\
\rho'_{13} = \rho'_{31} &\approx N_a N_b \frac{(P_{13} + \alpha_a \alpha_b P_{24}) \mathcal{E}_{1L} e^{-i(\omega_{12})t}}{\lambda_{31} - \hbar \omega_{12}}, \\
\rho'_{14} = \rho'_{41} &\approx \frac{N_a N_b (\alpha_a P_{24} - \alpha_b P_{13}) \mathcal{E}_{1L} e^{-i(\omega_{12})t}}{\lambda_{41} - \hbar \omega_{12}},
\end{aligned} \tag{16}$$

with all other $\rho_{ij} = 0$ and where we have defined

$$\begin{aligned}
\langle \hat{\mathbf{P}}(\omega_1) \rangle &= \frac{N_a^4 P_{12}^2 \mathcal{E}_{1R} (\hat{x} \cos \omega_1 t + \hat{y} \sin \omega_1 t)}{\lambda_{21} - \hbar \omega_{12}} + \frac{N_a^2 N_b^2 (P_{13} + \alpha_a \alpha_b P_{24})^2 \mathcal{E}_{1L} (\hat{x} \cos \omega_1 t - \hat{y} \sin \omega_1 t)}{\lambda_{31} - \hbar \omega_{12}} \\
&+ \frac{N_a^2 N_b^2 (\alpha_a P_{24} - \alpha_b P_{13})^2 \mathcal{E}_{1L} (\hat{x} \cos \omega_1 t - \hat{y} \sin \omega_1 t)}{\lambda_{41} - \hbar \omega_{12}}
\end{aligned} \tag{19}$$

This expression for the polarization is composed of several components which can be readily identified. The first term is the contribution to the polarization due to the allowed single-photon transition, 1–2, and interacts only with the right-hand circularly polarized component of the signal beam. Note, that this polarization is a function of the intensity of the control beam. The control beam produces energy-level shifts which cause λ_{21} to be modified. The polarization rotation effect produced by these level shifts will have to be properly included into any theory of the line shape obtained when using the effect for purposes of saturation spectroscopy.⁴

The second term interacts with only the left-hand polarized component and is made up of two parts. The first part results from the allowed, 1–3 single-photon transition, while the second is the polarization of a three-photon transition between levels 1 and 3. (Transitions involving more

$\lambda_{ij} = \lambda_i - \lambda_j$ and $\omega_{12} = \omega_1 - \omega_2$. Here, again, the antiresonant terms have been neglected. The polarization is obtained with the relationship

$$\langle \hat{\mathbf{P}} \rangle = \text{Tr}(\hat{\mathbf{p}} \rho), \tag{17}$$

where $\rho(t)$ is obtained from $\rho'(t)$ through the reverse transformations

$$\rho(t) = T^{-1} \rho'(t) T. \tag{18}$$

The result for that part of the polarization which oscillates at the frequency ω_1 is

than three photons are forbidden as a consequence of the rotating wave approximation.) The final term is responsible for two-photon transitions between levels 1 and 4, and it also interacts only with the left circularly polarized component of the signal beam. This two-photon term has two contributions which correspond to the two possible intermediate states which contribute to the two-photon transition. While we have included the possibility of two intermediate states in the calculation, there may only be one (for example if $3P_{1/2}$ is the dominant intermediate state) or there may be many. There may also be more than one possible final state (for example in the case of S – D two-photon transitions). These cases may be handled in the same general way, although numerical methods may be necessary.

If the control laser power is low we can expand Eq. (19) and obtain the following expression for $\hat{\mathbf{P}}$:

$$\begin{aligned}
\langle \hat{\mathbf{P}} \rangle &= \mathcal{E}_{1R} P_{12}^2 \left[\frac{1}{\hbar(\Omega_{21} - \omega_1)} - \frac{2P_{12}^2 \mathcal{E}_2^2}{\hbar^3(\Omega_{21} - \omega_1)(\Omega_{21} - \omega_2)} \left(\frac{1}{\Omega_{21} - \omega_1} + \frac{1}{\Omega_{21} - \omega_2} \right) \right] (\hat{x} \cos \omega_1 t + \hat{y} \sin \omega_1 t) \\
&+ \mathcal{E}_{1L} \left\{ P_{13}^2 \left[\frac{1}{\hbar(\Omega_{31} - \omega_1)} - \frac{P_{12}^2 \mathcal{E}_2^2}{\hbar^3(\Omega_{21} - \omega_2)(\Omega_{31} - \omega_1)} \left(\frac{1}{\Omega_{31} - \omega_1} + \frac{1}{\Omega_{21} - \omega_2} \right) \right] \right. \\
&\quad \left. + \frac{1}{\hbar} \left(\frac{P_{12} P_{42}}{\hbar(\Omega_{21} - \omega_2)} + \frac{P_{13} P_{43}}{\hbar(\Omega_{31} - \omega_1)} \right)^2 \frac{\mathcal{E}_2^2}{\Omega_{41} - (\omega_1 + \omega_2)} \right\} (\hat{x} \cos \omega_1 t - \hat{y} \sin \omega_1 t),
\end{aligned} \tag{20}$$

The rotation effect is proportional to the difference in the bulk susceptibilities for right and left circularly polarized light. This difference $\Delta\chi$ is equal to

$$\begin{aligned}
\Delta\chi &= N_{\text{eff}} \left\{ \frac{P_{12}^2 - P_{13}^2}{\hbar(\Omega_{21} - \omega_1)} - (2P_{12}^2 - P_{13}^2) \left[\frac{P_{12}^2 \mathcal{E}_2^2}{\hbar^3(\Omega_{21} - \omega_1)(\Omega_{21} - \omega_2)} \left(\frac{1}{\Omega_{21} - \omega_1} + \frac{1}{\Omega_{21} - \omega_2} \right) \right] \right. \\
&\quad \left. - \frac{1}{\hbar} \left(\frac{P_{12} P_{42}}{\hbar(\Omega_{21} - \omega_2)} + \frac{P_{13} P_{43}}{\hbar(\Omega_{31} - \omega_1)} \right)^2 \frac{\mathcal{E}_2^2}{\Omega_{41} - (\omega_1 + \omega_2)} \right\},
\end{aligned} \tag{21}$$

where N_{eff} is the effective atomic density for atoms in the ground state $|1\rangle$ and we have made use of the relationship $\Omega_{21} = \Omega_{31}$. This calculation must be repeated for each possible ground sublevel with the total difference susceptibility equal to the sum.

When $\omega_1 + \omega_2 \approx \Omega_{41}$, the effect of the two-photon dispersion dominates the level shifts and

$$\Delta\chi = -\frac{1}{\hbar^3} \left| \sum_{n, n'} \frac{P_{1n} P_{4n}}{\Omega_{n1} - \omega_1} + \frac{P_{1n'} P_{4n'}}{\Omega_{n'1} - \omega_2} \right|^2 \times \frac{\mathcal{E}_2^2}{\Omega_{41} - (\omega_1 + \omega_2)}, \quad (22)$$

where we have explicitly included a sum over all possible intermediate levels. (Levels $|n\rangle$ are connected to ground by $\Delta m_j = +1$ transitions where levels $|n'\rangle$ are connected to ground by $\Delta m_j = -1$ transitions.)

The angle of rotation, Φ , of the signal beam after traversing a cell of length L is given in radians by

$$\Phi = (\pi L \omega_1 / c) \Delta\chi. \quad (23)$$

The expressions for the polarization and susceptibility given above show two distinct resonances as a function of the control-laser frequency ω_2 . One resonance occurs when ω_2 is tuned near the ground state to intermediate state transition ($\omega_2 \approx \Omega_{21}$) since the level shifts are then maximized. The second resonance occurs at the two-photon resonance $\omega_1 + \omega_2 \approx \Omega_{41}$. No resonance is found in the region $\omega_2 \approx \Omega_{43}$ although one might expect one on the basis of the following. It has been shown that one can obtain large level shifts of levels 3 and 4 if the atoms are irradiated by a laser tuned near Ω_{43} . (See, for example, Ref. 14.) This shift of level 3 would be expected to produce an intensity dependent change in the susceptibility due to the 1-3 resonance transition, and this change would have a singularity at $\omega_2 \approx \Omega_{43}$. However, careful examination of a previous derivation¹⁰ of the two-photon transition reveals that two-photon transition matrix element also has a singularity at $\omega_2 \approx \Omega_{43}$ [see Eq. (18) or (35) of Ref. 10]. Apparently when both effects are taken into account, the effects of the shift of level 3 on the susceptibility are cancelled by this change in the two-photon transition such that no resonance occurs at $\omega_2 \approx \Omega_{43}$.

III. EXPERIMENTAL APPARATUS

The experimental set-up is schematically illustrated in Fig. 2. It consisted of two pulsed dye lasers which were pumped with a single nitrogen laser. The bandwidth of the signal laser was 0.1 Å while the control laser had about a 0.3-Å bandwidth. The outputs of the signal and control lasers were spatially filtered and passed through linear and circular polarizers, respectively, before they

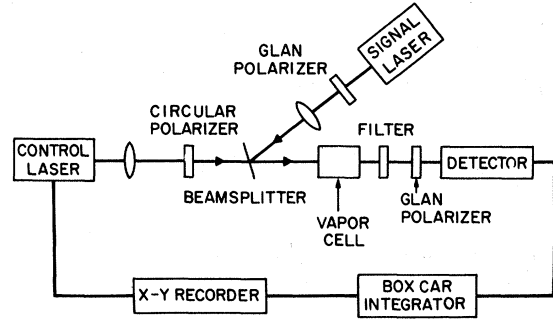


FIG. 2. Experimental set-up.

were combined and directed with a beamsplitter into the vapor cell. A stainless steel heat-pipe oven¹⁵ served to contain the vapor. At the low-sodium densities ($N \approx 3 \times 10^{14} \text{ cm}^{-3}$) which were used in our experiments, it was not possible to operate the oven in the heat-pipe mode, as several Torr of argon buffer gas was required to protect the oven windows. Thus all of the Na atoms were exposed to dephasing collisions from Ar atoms as well as other Na atoms. However, the resulting pressure broadening was small (on the order of a few natural linewidths) and thus had negligible effect.

Experiments were performed with both focused and collimated beams. In each case the diameter of the control laser beam was kept 2-3 times that of the signal beam in order that the signal beam would see a fairly uniform control intensity. With focused beams the control laser peak intensity inside the vapor cell was as high as $1.6 \times 10^7 \text{ W/cm}^2$ while that of the more tightly focused signal beam had a maximum peak intensity of $2.7 \times 10^5 \text{ W/cm}^2$. The focused beam waist radii of the control and signal beams were measured with a Reticon photodiode array and found to be $w_0 = 2.4 \times 10^{-2} \text{ cm}$ and $w_0 = 9.7 \times 10^{-3} \text{ cm}$, respectively. In the case of collimated beams, the control and signal beams had beam waist radii of $w_0 = 0.15$ and $w_0 = 0.05 \text{ cm}$ and peak-power densities of $4 \times 10^5 \text{ W/cm}^2$ and 10^4 W/cm^2 , respectively. In both cases, the power densities were often reduced by insertion of calibrated attenuators in either or both beams at locations before the combining beamsplitter.

After passing through the vapor cell, the signal beam was isolated with an interference filter and passed through an analyzing polarizer before detection with a silicon photodiode. The diode's output was processed with a boxcar averager and displayed on an x - y recorder whose x axis was driven by a potentiometer which was connected to the grating drive of the control laser.

The control-laser pulsewidth was approximately 6.5 nsec long while the signal laser pulsewidth

TABLE I. Relevant transition paths.

State	Path 1	Path 2	Path 3	Path 4
1	$3S_{1/2}(m = -\frac{1}{2})$	$3S_{1/2}(m = \frac{1}{2})$	$3S_{1/2}(m = -\frac{1}{2})$	$3S_{1/2}(m = \frac{1}{2})$
2	$3P_{3/2}(m = \frac{1}{2})$	$3P_{3/2}(m = \frac{3}{2})$	$3P_{1/2}(m = \frac{1}{2})$	
3	$3P_{3/2}(m = -\frac{3}{2})$	$3P_{3/2}(m = -\frac{1}{2})$		$3P_{1/2}(m = -\frac{1}{2})$
4	$5S_{1/2}(m = -\frac{1}{2})$	$5S_{1/2}(m = \frac{1}{2})$	$5S_{1/2}(m = -\frac{1}{2})$	$5S_{1/2}(m = \frac{1}{2})$

was only 4.5 nsec long. The optical paths from the lasers were adjusted such that the signal laser pulse arrived within the control-laser pulse and hence the rotation experienced by signal pulse was essentially constant in time. Thus the integrated pulse energy measurement made by the photodiode and boxcar were fairly accurate measures of the actual transmission through the polarizer.

IV. EXPERIMENTAL RESULTS

All of our experiments were conducted in Na vapor and utilized the 3S-5S two-photon transition. The signal laser was tuned near the 3S-3P fundamental transitions (between 5870 and 5910 Å) while the control-laser wavelength was tuned over the range from 6150 to 6300 Å. The relevant atomic-energy levels for the $m_j = \pm \frac{1}{2}$ ground states and for the $3P_{1/2}$ and $3P_{3/2}$ intermediate levels are given in Table I. The levels are labeled 1-4 in accordance with the theory given in Sec. II.

We initially observed polarization rotation effects with focused beams and with the signal laser tuned at 5891 Å, 1 Å from the $3P_{3/2}$ intermediate-state resonance. Figure 3 shows the sign and magnitude of the angle of rotation as a function of detuning from exact two-photon resonance. In this experiment, the angle of rotation

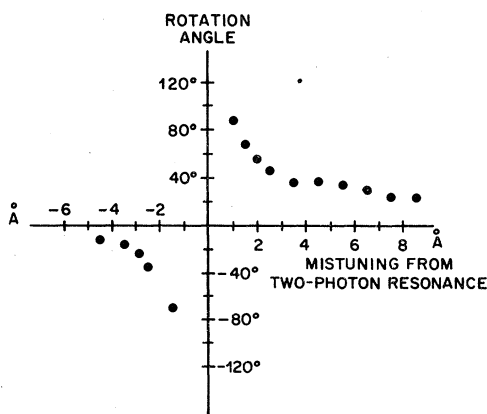


FIG. 3. Rotation angle vs control laser wavelength, in terms of mistuning from two-photon resonance. Signal laser tuned at 5890.6 Å and control-laser intensity is 1.3×10^6 W/cm².

was determined by rotating the analyzing polarizer, the mistuning from the two-photon resonance was varied by tuning the control laser, and the control-laser intensity was maintained at a constant 1.3×10^6 W/cm². The behavior of the angle of rotation is clearly in qualitative agreement with the dispersion associated with the two-photon resonance line. The asymmetry between the short- and long-wavelength sides of the line, which we had attributed to self-focusing and self-defocusing effects in an earlier publication,¹ will be shown later in this paper to be a consequence of the level shifts.

The dependence of the rotation angle on control-beam intensity was also measured. The signal laser was tuned at 5891 Å and the control laser at 6159 Å, i.e. 1 Å from both the $3P_{3/2}$ intermediate-state resonance and $3S_{1/2}$ - $5S_{1/2}$ two-photon resonance. Figure 4 shows the rotation angle and the transmission through a crossed polarizer as functions of the control-beam intensity. The angle is seen to be linearly proportional to the control-laser intensity with a slope of 3.1×10^{-5} deg/(W/cm²). Since the mistuning from two-photon resonance is small, level shifts are not important, and Eqs. (23) and (22) may be used to obtain a calculated slope of 1.6×10^{-5} deg/

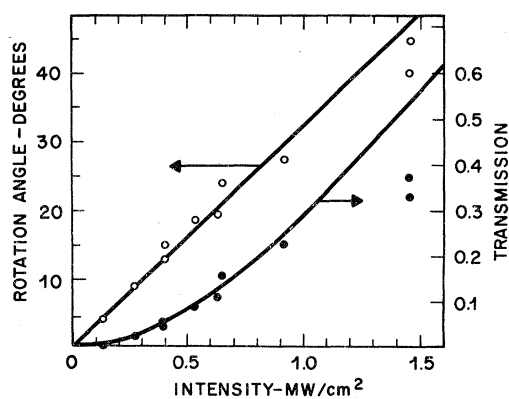


FIG. 4. Intensity dependence of rotation angle and transmission through crossed polarizer. Control and signal dye lasers tuned such that the mistuning from both the single-photon intermediate state resonance and the two-photon resonance is 1 Å.

(W/cm^2). (This calculation employed dipole matrix elements derived from tabulated values for $3S-3P$ and $3P-5S$ oscillator strengths.) In view of the uncertainties involved in our measurements, experiment and theory are in good agreement.

We repeated our measurement of the dispersion of the angle of rotation using an analyzing polarizer set to be crossed to the initial signal-laser polarization. The transmission through this polarizer was plotted vs the frequency of the control laser on an x - y recorder. Figure 5 shows the transmission observed as the control laser was tuned over 150 \AA . The signal-laser wavelength was 5888.7 \AA . Two features are to be noticed. First, the transmission decreases at exact two-photon resonance due to strong two-photon absorption. Second, the transmission is clearly asymmetric about the two-photon resonance with the signal dropping to zero at a control-laser wavelength of approximately 6150 \AA . This asymmetry is produced by an interference between the effects of the two-photon transition and the effects of the level shift on the single-photon resonance transition. Figure 6 shows an expanded view. The line curve in Fig. 6 is a calculated curve using Eqs. (21) and (23) which was obtained with no adjustable parameters except for a normalization factor. This type of interference effect between two different contributions to the susceptibility is quite striking and provides direct confirmation for the ratio of the $3S-3P$ and $3P-5S$ oscillator strengths. Similar interference effects between distinct contributions to a nonlinear susceptibility have recently been observed by Lotem and Lynch.¹⁶

Figure 7 shows data obtained with collimated beams and the analyzing polarizer again set such that it is crossed to the initial signal-laser polarization. The transmission through this polarizer is plotted vs the frequency of the control laser.

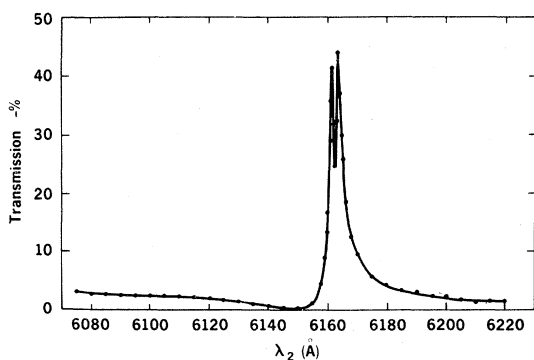


FIG. 5. Transmission of signal beam through crossed polarizer. Signal laser tuned at 5888.7 \AA . Control-laser intensity is $1.5 \times 10^6 \text{ W}/\text{cm}^2$. Line is drawn through data points to aid the eye in following data.

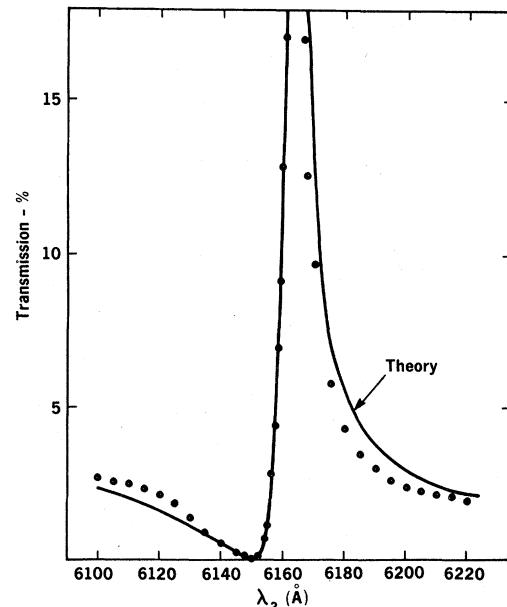


FIG. 6. Transmission of signal beam through crossed polarizer. Experimental conditions as in Fig. 5. Points are experimental; solid line is theory as given in text.

Several traces are shown corresponding to different wavelengths of the signal laser. Two resonances are found. One resonance occurs at the $3P_{3/2}-5S_{1/2}$ transition frequency while the second, which corresponds to the two-photon resonance, occurs at $\Omega - \omega_2$, where $\hbar\Omega$ is the energy separation $3S-5S$ and ω_2 is the frequency of the control laser.

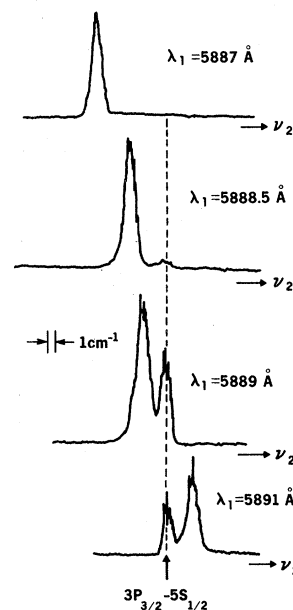


FIG. 7. Transmission of signal through crossed polarizer vs control laser frequency for several signal wavelengths. Control laser intensity is about $10^6 \text{ W}/\text{cm}^2$. Vertical scale is not the same for each run.

The vertical scale for each trace is different. The signals increase rapidly as the signal laser is tuned closer to the $3P$ intermediate state resonances. Figure 8 contains data which illustrate the resonant enhancement¹⁷ obtained when one tunes the signal laser close to the intermediate state. The vertical axis corresponds to the peak two-photon rotation signal normalized to the square of the control intensity (the signals were always kept small enough such that $\sin^2\Phi \approx \Phi^2$), while the horizontal axis is the signal laser wavelength. The solid line is calculated with no adjustable parameters other than an overall normalization factor. (Since the detunings from exact two-photon resonance are small, level shifts may be neglected.) The agreement between theory and experiment is satisfactory, but not as good as would appear from the figure. Although we chose to normalize to the square of the control intensity, as dictated by theory, we noticed that in this case, with exact two-photon resonance, the experimental signal increased slightly more slowly than I_c^2 . The discrepancy between this power dependence and the theory is not completely understood. It may arise from a partial saturation of the two-photon resonance. This discrepancy was not observed when tuned off of two-photon resonance as shown in Fig. 4.

The spectra shown in Fig. 7 clearly demonstrate that the rotation effect may serve as a sensitive technique for detection of two-photon resonances. If this data had been obtained with narrow-band

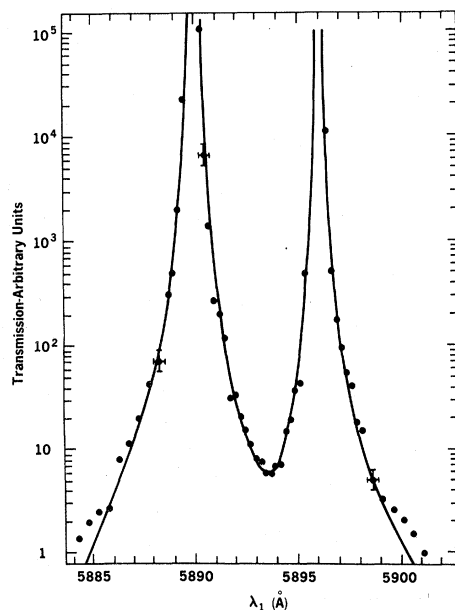


FIG. 8. Normalized transmission of signal at exact two-photon resonance through crossed polarizer vs wavelength of signal laser.

lasers and oppositely propagating beams, Doppler-free spectra¹⁸ could have been obtained. The two-photon resonance observed with this rotation technique is a result of both the real and imaginary parts of the two-photon susceptibility. It is easily shown that in the limit of low intensities, the intensity which passes through an initially crossed polarizer is given by

$$I = (4\pi)^2 I_0 (\Delta\eta^2 + \Delta\alpha^2) l^2, \quad (24)$$

where I_0 is the intensity of the signal laser, and $\Delta\eta$ and $\Delta\alpha$ are the differences of the real and imaginary parts, respectively, of the complex susceptibility for right and left circularly polarized light. Note that $\Delta\alpha$ and $\Delta\eta$ are related by Kramers-Kronig relationships so if $\Delta\alpha$ were Lorentzian, as would be the case for Doppler-free two-photon spectroscopy, then the signal given in Eq. (24) is also Lorentzian.

By setting the analyzing polarizer at some angle, θ away from the perfectly crossed position, one can obtain a signal which is essentially proportional to $\Delta\eta$ alone. In this case one obtains

$$I = I_0 [\theta^2 - 4\Delta\eta l\theta + (\Delta\eta^2 + \Delta\alpha^2) l^2] \\ \approx I_0 (\theta^2 - 4\Delta\eta l\theta). \quad (25)$$

Figure 9 shows the evolution of the signal as the analyzing polarizer is rotated away from the crossed position, and illustrates how a dispersive signal is obtained.

Detection of two-photon resonances is often accomplished by monitoring the fluorescence which

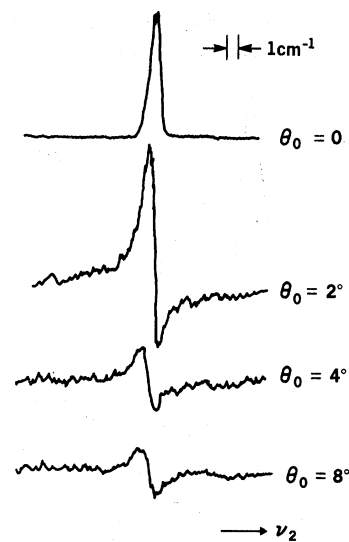


FIG. 9. Dependence of signal transmission on angle of analyzing polarizer. Vertical scale and zero differ for each angle. The noise is due to shot-to-shot fluctuations in laser power.

results from the two-photon excited state. However, in some cases this fluorescence may be very weak or masked by a strong background as in the case of a discharge and therefore may be difficult to observe. In this case one must detect the change in transmission due to the two-photon resonances which usually result in a very low signal to background ratio. The signal to background ratio for spectra obtained with the rotation effect is

$$R = 4 \Delta \eta l \theta / (\theta^2 + \phi^2), \quad (26)$$

where ϕ^2 is the extinction coefficient of the polarizers. This expression maximizes at $\theta = \phi$, and hence with good polarizers, excellent values for R can be obtained.

Whereas the two-photon resonances observed in Fig. 7 are to be clearly expected, the resonances at the $3P_{3/2} - 5S_{1/2}$ frequency would not be expected on the basis of the discussion given in Sec. II. This additional resonance is a collision-induced signal. The $3P_{3/2}$ state is actually populated by absorption of signal laser photons. Collisions are required since the signal laser is not resonant with the $3S_{1/2} - 3P_{3/2}$ transition. By reducing the buffer gas pressure we can virtually eliminate this resonance. The effect of the control laser is to modify the population of certain m_j sublevels of the $3P_{3/2}$ state by causing transitions to $5S_{1/2}$. This change in population causes the dispersion of the $3S_{1/2} - 3P_{3/2}$ resonance transition to be different for right and left circularly polarized light and hence a rotation in the signal polarization. In Fig. 10 we show the signal as it is observed through a slightly uncrossed polarizer. The two-photon resonance has a dispersion shape. The other

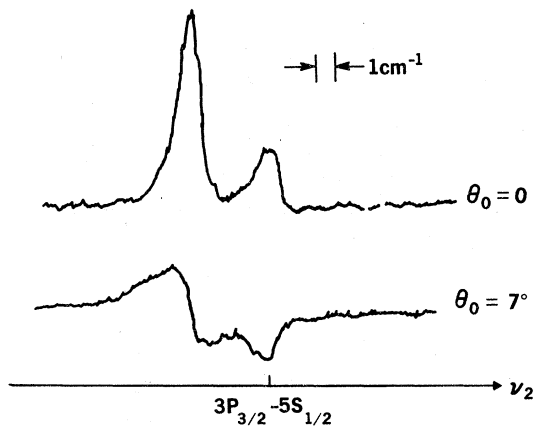


FIG. 10. Signal transmission vs control-laser frequency through crossed polarizer and through polarizer at 7° . Signal laser wavelength is 5888.8, control-laser intensity is 10^3 W/cm 2 , signal-laser intensity is 10^4 W/cm 2 .

resonance has the shape of an absorption causing transitions between $3P_{3/2}$ and $5S_{1/2}$.

V. DISCUSSION

Two important figures of merit of an optical switch are the peak transmission and the extinction rate of the device. The data given in Fig. 5 show a peak transmission of about 45%, however we have been able to obtain transmissions as high as 70%. The extinction obtained with the switch in the "off" position (i.e., in the absence of the control beam) was limited by quality of the glan polarizers. For signal wavelengths in the immediate vicinity of the D_1 resonance line, we found that the signal beam became strongly depolarized. This depolarization is due to an ellipse rotation effect and will be the subject of a future publication. With the exception of this region, the extinction was generally 10^{-5} . It should be noted that for the conditions of Fig. 5, we observed strong self-defocusing of the signal beam. The index change which produces the defocusing is due to the nonlinearity of the $3S - 3P$ single-photon resonances and is of the same order as the rotation effect. Hence, the focusing or defocusing effects can be reduced by increasing the beam diameters, while keeping the control intensity constant to provide the same rotation angle. Such an increase was not possible in our experiments since our control-laser power was limited. The focusing or defocusing effects can also be reduced by operating at a signal wavelength further from the $3S - 3P$ intermediate state resonance.

The speed at which an optical shutter utilizing the rotation effect opens or closes is determined only by the temporal characteristics of the control-laser pulse. One must, however, operate at wavelengths which are sufficiently removed from the two-photon resonances such that all spectral components of the pulses produce the same rotation.

Figure 8 clearly illustrates the benefit obtained by using a nearly resonant intermediate state. However, it does not necessarily imply that such a resonance is required. If one must operate at a wavelength for which no nearly resonant intermediate state exists, one should increase either the density of the atomic vapor or the control-laser power level. Note that both of these parameters can be increased significantly since we will not experience either the loss or the nonlinear effects such as self-focusing associated with a nearly resonant intermediate state.

Gases possess the advantageous properties of tolerance to high optical-power densities, of transparency over wide ranges of the electromag-

netic spectrum, and of ease of scaling to arbitrary dimensions. By choosing the atomic system and the frequency of the control beam appropriately, it should be possible to control beams from the far-infrared to the vacuum ultraviolet.

For the purposes of spectroscopy the rotation effect provides a sensitive technique for detection of two-photon absorption spectra with high signal to background ratio. When compared with direct measurement of the attenuation produced by two-photon absorption, one improves the signal to background ratio by approximately the square root of the extinction ratio of the polarizers used. The rotation also provides a direct measurement of the two-photon cross section if one is able to accurately determine the vapor density and control-laser power. Interference effects between different contributions to the rotation such as

were observed, can give very accurate values for relative cross sections or oscillation strengths.

The concept of two-photon dispersion which is utilized in these experiments can also be applied to many other phenomena such as self-focusing¹⁹ and self-phase-modulation.²⁰ Two-photon group velocity dispersion should be useful for pulse compression. Many new applications can be expected in the future.

ACKNOWLEDGMENTS

The authors wish to thank J. E. Bjorkholm for helpful conversations and J. P. Gordon for many discussions which clarified the cancellation of the effects of the two-photon dispersion by the optically induced level shifts.

¹P. F. Liao and G. C. Bjorklund, *Phys. Rev. Lett.* **36**, 584 (1976).

²V. M. Arutyunyan, T. A. Papazyan, G. G. Adonts, A. V. Karmenyan, S. P. Ishkhanyan, and L. Khol'ts, *Zh. Eksp. Teor. Fiz.* **68**, 44 (1975) [*Sov. Phys.-JETP* **41**, 22 (1976)].

³D. Heiman, R. W. Hellwarth, M. D. Levenson, and G. Martin, *Phys. Rev. Lett.* **36**, 189 (1976).

⁴C. Wieman and T. W. Hänsch, *Phys. Rev. Lett.* **36**, 1170 (1976).

⁵The concept of controlling the dielectric constant for one light beam with a second switching beam has also been introduced by J. A. Armstrong and D. Grischkowsky, U. S. Patent No. 3864 020 (1975), although the role of the two-photon resonance was not realized at the time.

⁶B. Cagnac, G. Grynberg, and F. Biraben, *J. Phys. (Paris)* **34**, 845 (1973).

⁷See, for example, D. Grischkowsky, *Phys. Rev. Lett.* **25**, 566 (1974); J. E. Bjorkholm, E. H. Turner, and D. B. Pearson, *Appl. Phys. Lett.* **26**, 564 (1975); H. M. Gibbs, G. C. Churchill and G. J. Salamo, *Opt. Commun.* **12**, 396 (1974); and M. T. Loy, *Appl. Lett.* **26**, 99 (1974).

⁸A. M. Bonch-Bruevich, N. N. Kostin, and V. A. Kho-

dovoi, *Zh. Eksp. Teor. Fiz. Pis'ma Red.* **3**, 425 (1966) [*JETP Lett.* **3**, 279 (1966)].

⁹See Ref. 10 and work cited therein.

¹⁰D. Grischkowsky, M. M. T. Loy, and P. F. Liao, *Phys. Rev. A* **12**, 2514 (1975).

¹¹D. Grischkowsky, *Phys. Rev. A* **14**, 802 (1976).

¹²C. Cohen-Tannoudji and S. Haroche, *J. Phys. (Paris)* **30**, 153 (1969).

¹³D. Bohm, *Quantum Theory* (Prentice Hall, Englewood Cliffs, New Jersey, 1951), p. 448.

¹⁴P. F. Liao and J. E. Bjorkholm, *Opt. Commun.* **16**, 392 (1976).

¹⁵C. R. Vidal and J. Cooper, *J. Appl. Phys.* **40**, 3370 (1969).

¹⁶H. Lotem and R. T. Lynch, Jr., *Phys. Rev. Lett.* **37**, 334 (1976).

¹⁷J. E. Bjorkholm and P. F. Liao, *Phys. Rev. Lett.* **33**, 128 (1974).

¹⁸L. S. Vasilenko, V. P. Chebotaev, and A. V. Shishaev, *Zh. Eksp. Teor. Fiz. Pis'ma Red.* **12**, 161 (1970) [*JETP Lett.* **12**, 113 (1970)].

¹⁹R. H. Lehmberg, J. Reintjes, and R. C. Eckhardt, *Appl. Phys. Lett.* **25**, 374 (1974).

²⁰R. H. Lehmberg, J. Reintjes, and R. C. Eckhardt, *Opt. Commun.* **18**, 174 (1976).